

# Pseudogap phase formation in the crossover from Bose–Einstein condensation to BCS superconductivity

V. P. Gusynin<sup>1\*</sup>, V. M. Loktev<sup>1†</sup> and S. G. Sharapov<sup>2‡</sup>

<sup>1</sup>*Bogolyubov Institute for Theoretical Physics,  
252143 Kiev, Ukraine*

<sup>2</sup>*Department of Physics, University of Pretoria,  
0002 Pretoria, South Africa*

(June 3, 1998)

## Abstract

A phase diagram for a 2D metal with variable carrier density has been derived. It consists of a normal phase, where the order parameter is absent; a so-called “abnormal normal” phase where this parameter is also absent but the mean number of composite bosons (bound pairs) exceeds the mean number of free fermions; a pseudogap phase where the absolute value of the order parameter gradually increases but its phase is a random value, and finally a superconducting (here Berezinskii–Kosterlitz–Thouless) phase. The characteristic transition temperatures between these phases are found. The chemical potential and paramagnetic susceptibility behavior as functions of the fermion density and the temperature are also studied. An attempt is made to qualitatively compare the resulting phase diagram with the features of underdoped high- $T_c$  superconducting compounds above their critical temperature.

PACS: 74.72.-h, 74.20.Fg, 74.20.Mn, 64.60.Cn

## I. INTRODUCTION

The study of the crossover region between superconductivity of Cooper pairs and superfluidity of composite bosons is attracting much attention due to its close relationship to the problem of describing high-temperature superconductors (HTSC) (see, e.g., Refs. [1–3]). At present this region is understood for 3D systems, both at zero and finite temperatures [4,5]. The crossover in quasi-2D systems has also been studied [6], albeit only partially, whereas for 2D systems only the case of  $T = 0$  has been studied thoroughly [4,7]. This is related to the fact that fluctuations of the charged complex order parameter in 2D systems are so large that they destroy long-range order at any finite temperature (Coleman–Mermin–Wagner–Hohenberg (CMWH) theorem [8]). In this case the appearance of an inhomogeneous condensate with a power-law decay for the correlations (the so-called Berezinskii–Kosterlitz–Thouless (BKT) phase) is possible. However an adequate mathematical description for BKT phase formation is still lacking.

Most previous analyses [9–11] of the behavior of 2D systems at  $T \neq 0$  have been based on the Nozières–Schmitt–Rink approach [12]. This approach is simply a Gaussian approx-

imation to the functional integral, and this perhaps explains the difficulties faced in these calculations. On the one hand, Gaussian fluctuations destroy long-range order in 2D, and if one searches for the  $T_c^{2D}$  at which order sets in, one should obtain zero in accordance with the aforementioned theorems [8]. On the other hand, taking Gaussian fluctuations into account is completely inadequate to describe the BKT transition [13].

Nonetheless, there has been some progress. For example, the BKT transition has been studied in relativistic  $2 + 1$ -theory [14], and the crossover from superconductivity to superfluidity has been considered [15] as a function of the carrier density  $n_f$  (see also Ref. [16]). However, the method employed in Ref. [15] to obtain the temperature  $T_{\text{BKT}}$  has several drawbacks. Most importantly, the equation for  $T_{\text{BKT}}$  was obtained without considering the existence of a neutral (real) order parameter  $\rho$ , whose appearance at finite  $T$  does not violate the CMWH theorem.

As we show below,  $\rho$  defines the modulus of a multivalued complex order parameter  $\Phi$  for a 2D system. As a result of allowing for a neutral order parameter, a region where  $\rho$  decays gradually to zero appears in the phase diagram of the system. This region separates the standard normal phase with  $\rho = 0$  from the BKT phase, where the correlations exhibit power-law decay. Despite the exponential decay of correlations, this new region of states may be expected to possess unusual properties, since  $\rho$  plays the same role as the energy gap  $\Delta$  in the theory of ordinary superconductors in many cases.<sup>1</sup> The possible existence of such a phase, which in some sense is also normal, may shed light on the anomalous behavior of the normal state of HTSC (see, for example, the reviews in Refs. [1,2] and [18]). In particular, the temperature dependencies of the spin susceptibility, resistivity, specific heat, photoemission spectra, and other quantities [2,19] can be explained by the formation of either a pseudogap or a spin gap in the region  $T > T_c$ .

Using a very simple continuum 2D model, this approach was first attempted in a brief note [20], where we calculated  $T_{\text{BKT}}$  and  $T_\rho$  ( $T_\rho$  is the temperature defined by the condition  $\rho = 0$ ) self-consistently as functions of  $n_f$ , and established the boundaries of this new *pseudogap* region, which lies between  $T_{\text{BKT}}$  and  $T_\rho$ .

The purpose of this article is to develop this approach further. Using the static paramagnetic susceptibility as an example, we demonstrate that the pseudogap opens below  $T_\rho$ . Furthermore, we analyze the difference between the commonly used (see Refs. [3] and [4]) pairing temperature  $T_P$  and the temperature  $T_\rho$  introduced here. These temperatures turn out to be different if the chemical potential  $\mu < 0$ . We also introduce here an *abnormal normal* phase, which lies between  $T_P$  and  $T_\rho$ , where preformed bosons exist. This more detailed study helps to clarify the physical import of  $T_\rho$ , as well as the nature of the transition at  $T_\rho$ . It was believed in the related model [14] that this is a second-order phase transition. We argue however, that fluctuations in the phase of the order parameter can transform the transition to a crossover, as observed experimentally.

In Sec. II we present the model and the relevant formalism. The equations for  $T_{\text{BKT}}$ ,  $\rho$ ,  $T_\rho$ , and the chemical potentials  $\mu(T_{\text{BKT}})$  and  $\mu(T_\rho)$  are derived in Sec. III. Since the technique

---

<sup>1</sup> To calculate the observed single-particle spectrum, of course, carrier losses due to scattering of carriers by fluctuations of the phase of the order parameter (and in real systems by dopants) must be taken into account; see Ref. [17].

employed to obtain the equation for  $T_{\text{BKT}}$  is not widely used, we consider it useful to present a detailed derivation of this equation. (The details of the calculation of the effective potential and useful series are given in Appendix A.) The systems of equations for  $T_{\text{BKT}}$ ,  $\rho(T_{\text{BKT}})$ ,  $\mu(T_{\text{BKT}})$  and  $T_\rho$ ,  $\mu(T_\rho)$  are analyzed in Sec. IV. The difference between pairing temperature  $T_P$  and the temperature  $T_\rho$  is discussed in Sec. V. Also discussed is the physical import of  $T_\rho$ . Using the example of the static spin susceptibility, it is shown in Sec. VI that the resulting pseudogap phase can in fact be used to explain the aforementioned anomalous properties of HTSC.

## II. THEORETICAL FRAMEWORK

The simplest model Hamiltonian density for fermions confined to a 2D volume  $v$  is [4,7,9]

$$\mathcal{H} = \psi_\sigma^\dagger(x) \left( -\frac{\nabla^2}{2m} - \mu \right) \psi_\sigma(x) - V \psi_\uparrow^\dagger(x) \psi_\downarrow^\dagger(x) \psi_\downarrow(x) \psi_\uparrow(x), \quad (2.1)$$

where  $x \equiv \mathbf{r}, \tau$ ;  $\psi_\sigma(x)$  is a fermion field,  $m$  is the effective fermion mass,  $\mu$  is the chemical potential, and  $V$  is an effective local attraction constant; we take  $\hbar = k_B = 1$ .

The Hubbard–Stratonovich method, which is standard for these problems [21], can be applied to write the partition function  $Z(v, \mu, T)$  as a functional integral over Fermi fields (Nambu spinors) and the auxiliary field  $\Phi = V \psi_\uparrow^\dagger \psi_\downarrow^\dagger$ . In contrast to the usual method for calculating  $Z$  in  $\Phi$ ,  $\Phi^*$  variables, the parametrization  $\Phi(x) = \rho(x) \exp[-i\theta(x)]$  is more appropriate for presenting the corresponding integral in two dimensions [22] (see also Refs. [23] and [24]). When this replacement by modulus–phase variables is implemented, it is evident that one must also replace  $\psi_\sigma(x) = \chi_\sigma(x) \exp[i\theta(x)/2]$ . Physically, this amounts to replacing the charged fermion  $\psi_\sigma(x)$  with a neutral fermion  $\chi_\sigma(x)$  and spinless charged boson  $e^{i\theta(x)/2}$ . Note that while one may formally use any self-consistent definition of the new variables, the physical condition that the macroscopic variable  $\Phi(x)$  be single-valued under  $2\pi$  rotations fixes the parametrization. This was not taken into account in Ref. [20], where a different parametrization was used.

As a result, one obtains

$$Z(v, \mu, T) = \int \rho \mathcal{D}\rho \mathcal{D}\theta \exp[-\beta\Omega(v, \mu, T, \rho(x), \partial\theta(x))], \quad (2.2)$$

where

$$\beta\Omega(v, \mu, T, \rho(x), \partial\theta(x)) = \frac{1}{V} \int_0^\beta d\tau \int d\mathbf{r} \rho^2(x) - \text{Tr} \ln G^{-1} + \text{Tr} \ln G_0^{-1} \quad (2.3)$$

is the one-loop effective action, which depends on the modulus–phase variables. The action (2.3) can be expressed in terms of the Green function of the initial (charged) fermions, which in the new variables has the operator form

$$\begin{aligned} G^{-1} = & -\hat{I}\partial_\tau + \tau_3 \left( \frac{\nabla^2}{2m} + \mu \right) + \tau_1 \rho(\tau, \mathbf{r}) \\ & - \tau_3 \left[ \frac{i\partial_\tau \theta(\tau, \mathbf{r})}{2} + \frac{(\nabla \theta(\tau, \mathbf{r}))^2}{8m} \right] + \hat{I} \left[ \frac{i\nabla^2 \theta(\tau, \mathbf{r})}{4m} + \frac{i\nabla \theta(\tau, \mathbf{r}) \nabla}{2m} \right]. \end{aligned} \quad (2.4)$$

The free fermion Green function  $G_0 = G|_{\mu, \rho, \theta=0}$  provides a convenient regularization in the process of calculation. It is important that neither the smallness nor slowness of the variation of the phase of the order parameter is assumed in obtaining expression (2.3). In other words, it is formally exact.

Since the low-energy dynamics of phases for which  $\rho \neq 0$  is governed mainly by long-wavelength fluctuations of  $\theta(x)$ , only the lowest-order derivatives of the phase need be retained in the expansion of  $\Omega(v, \mu, T, \rho(x), \partial\theta(x))$ :

$$\Omega(v, \mu, \rho(x), \partial\theta(x)) \simeq \Omega_{\text{kin}}(v, \mu, T, \rho, \partial\theta(x)) + \Omega_{\text{pot}}(v, \mu, T, \rho), \quad (2.5)$$

where

$$\Omega_{\text{kin}}(v, \mu, T, \rho, \partial\theta(x)) = T \text{Tr} \sum_{n=1}^{\infty} \frac{1}{n} (\mathcal{G}\Sigma)^n \Big|_{\rho=\text{const}} \quad (2.6)$$

and

$$\Omega_{\text{pot}}(v, \mu, T, \rho) = \left( \frac{1}{V} \int d\mathbf{r} \rho^2 - T \text{Tr} \ln \mathcal{G}^{-1} + T \text{Tr} \ln G_0^{-1} \right) \Big|_{\rho=\text{const}}. \quad (2.7)$$

The kinetic  $\Omega_{\text{kin}}$  and potential  $\Omega_{\text{pot}}$  parts can be expressed in terms of the Green function of the neutral fermions, which satisfies the equation

$$\left[ -\hat{I} \partial_{\tau} + \tau_3 \left( \frac{\nabla^2}{2m} + \mu \right) + \tau_1 \rho \right] \mathcal{G}(\tau, \mathbf{r}) = \delta(\tau) \delta(\mathbf{r}), \quad (2.8)$$

and the operator

$$\Sigma(\partial\theta) \equiv \tau_3 \left[ \frac{i \partial_{\tau} \theta}{2} + \frac{(\nabla \theta)^2}{8m} \right] - \hat{I} \left[ \frac{i \nabla^2 \theta}{4m} + \frac{i \nabla \theta(\tau, \mathbf{r}) \nabla}{2m} \right]. \quad (2.9)$$

The representation (2.5) enables one to obtain the full set of equations necessary to find  $T_{\text{BKT}}$ ,  $\rho(T_{\text{BKT}})$ , and  $\mu(T_{\text{BKT}})$  at given  $\epsilon_F$  (or, for example,  $\rho(T)$  and  $\mu(T)$  at given  $T$  and  $\epsilon_F$ ). While the equation for  $T_{\text{BKT}}$  will be written using the kinetic part (2.6) of the effective action, the equations for  $\rho(T_{\text{BKT}})$  and  $\mu(T_{\text{BKT}})$  (or  $\rho(T)$  and  $\mu(T)$ ) can be obtained using the mean field potential (2.7). It turns out that at a phase for which  $\rho \neq 0$ , the mean-field approximation for the modulus variable describes the system quite well. This is mainly related to the nonperturbative character of the Hubbard–Stratonovich method, i.e., most effects carry over for a nonzero value of  $\rho$ .

It is clear that the CMWH theorem does not preclude nonzero  $\langle \rho \rangle$  and, as a consequence, an energy gap for fermion  $\chi$ , since no continuous symmetry is broken when such a gap appears. Despite strong phase fluctuations in the two-dimensional case, the energy gap in the spectrum of the neutral fermion  $\chi$  can still persist in the spectrum of the charged fermion  $\psi$  [22], even well above the critical temperature.<sup>2</sup> We believe that the pseudogap widely

---

<sup>2</sup> We note that the specific heat experiments [2] demonstrated the loss of entropy that occurs at temperatures much higher than  $T_c$ . This can be considered indicative of a degenerate normal state, consistent with the existence of a nonzero order parameter  $\langle \rho \rangle$ .

discussed in high- $T_c$  cuprates might be attributable to the energy gap of a neutral fermion introduced in the way described above, so that the pseudogap itself can be considered a remnant of the superconducting gap. The condensate of neutral fermions has nothing to do with the superconducting transition; the latter is only possible when the superfluid density of bosons becomes large enough to stiffen the phase  $\theta(x)$ . The temperature  $T_\rho$  at which nonzero  $\langle \rho \rangle$  develops should be identified in this approach with the pseudogap onset temperature [2,19]. The strategy of treating charge and spin degrees of freedom as independent seems to be quite useful, and at the same time a very general feature of two-dimensional systems.

### III. DERIVATION OF SELF-CONSISTENT EQUATIONS FOR $T_{\text{BKT}}$ , NEUTRAL ORDER PARAMETER, AND CHEMICAL POTENTIAL

If the model under consideration is reduced to some known model describing the BKT phase transition, one can easily write the equation for  $T_{\text{BKT}}$ , which in the present approach can be identified with the superconducting transition temperature  $T_c$ . Indeed, in the lowest orders the kinetic term (2.6) coincides with the classical spin XY-model [25,26], which has the continuum Hamiltonian

$$\mathcal{H} = \frac{J}{2} \int d\mathbf{r} [\nabla\theta(\mathbf{r})]^2. \quad (3.1)$$

Here  $J$  is the some coefficient (in the original classical discrete XY-model it is the stiffness of the relatively small spin rotations) and  $\theta$  is the angle (phase) of the two-component vector in the plane.

The temperature of the BKT transition is, in fact, known for this model:

$$T_{\text{BKT}} = \frac{\pi}{2} J. \quad (3.2)$$

Despite the very simple form<sup>3</sup> of Eq. (3.2), it was derived (see, e.g., Refs. [25] and [26]) using the renormalization group technique, which takes into account the non-single-valuedness of the phase  $\theta$ . Thus, fluctuations of the phase are taken into account in a higher approximation than Gaussian. The XY-model was assumed to be adequate for a qualitative description of the underdoped cuprates [27] (see also Ref. [28]), and the relevance of the BKT transition to Bose- and BCS-like superconductors was recently discussed in Ref. [16].

To expand  $\Omega_{\text{kin}}$  up to  $\sim (\nabla\theta)^2$ , it is sufficient to restrict ourselves to terms with  $n = 1, 2$  in the expansion (2.6). The calculation is similar to that employed in Ref. [29], where only high densities  $n_f$  were considered at  $T = 0$ . Thus, to obtain the kinetic part, one should directly calculate the first two terms of the series (2.6), which can be formally written  $\Omega_{\text{kin}}^{(1)} = T\text{Tr}(\mathcal{G}\Sigma)$  and  $\Omega_{\text{kin}}^{(2)} = \frac{1}{2}T\text{Tr}(\mathcal{G}\Sigma\mathcal{G}\Sigma)$ . We note that  $\Sigma$  has the structure  $\Sigma = \tau_3 O_1 + \hat{I} O_2$ , where  $O_1$  and  $O_2$  are differential operators (see (2.9)). One can see, however, that the part of  $\Sigma$  proportional to the unit matrix  $\hat{I}$  does not contribute to  $\Omega_{\text{kin}}^{(1)}$ . Hence,

---

<sup>3</sup>An exponentially small correction is omitted here.

$$\Omega_{\text{kin}}^{(1)} = T \int_0^\beta d\tau \int d\mathbf{r} \frac{T}{(2\pi)^2} \sum_{n=-\infty}^{\infty} \int d\mathbf{k} \text{Tr}[\mathcal{G}(i\omega_n, \mathbf{k})\tau_3] \left( \frac{i\partial_\tau\theta}{2} + \frac{(\nabla\theta)^2}{8m} \right), \quad (3.3)$$

where

$$\mathcal{G}(i\omega_n, \mathbf{k}) = -\frac{i\omega_n \hat{I} + \tau_3 \xi(\mathbf{k}) - \tau_1 \rho}{\omega_n^2 + \xi^2(\mathbf{k}) + \rho^2} \quad (3.4)$$

is the Green function of neutral fermions in the frequency-momentum representation, with  $\xi(\mathbf{k}) = \varepsilon(\mathbf{k}) - \mu$  and  $\varepsilon(\mathbf{k}) = \mathbf{k}^2/2m$ .

The summation over the Matsubara frequencies  $\omega_n = \pi(2n+1)T$  and integration over  $\mathbf{k}$  in (3.3) can be easily performed using the sum (A.7); one thus obtains

$$\Omega_{\text{kin}}^{(1)} = T \int_0^\beta d\tau \int d\mathbf{r} n_F(\mu, T, \rho) \left( \frac{i\partial_\tau\theta}{2} + \frac{(\nabla\theta)^2}{8m} \right), \quad (3.5)$$

where

$$n_F(\mu, T, \rho(\mu, T)) = \frac{m}{2\pi} \left\{ \sqrt{\mu^2 + \rho^2} + \mu + 2T \ln \left[ 1 + \exp \left( -\frac{\sqrt{\mu^2 + \rho^2}}{T} \right) \right] \right\}. \quad (3.6)$$

This has the form of a Fermi quasiparticle density (for  $\rho = 0$  the expression (3.6) is simply the density of free fermions).

For the case  $T = 0$  [23,29], in which real time  $t$  replaces imaginary time  $\tau$ , one can argue from Galilean invariance that the coefficient of  $\partial_t\theta$  is rigorously related to the coefficient of  $(\nabla\theta)^2$ . It therefore does not appear in  $\Omega_{\text{kin}}^{(2)}$ . We wish, however, to stress that these arguments cannot be used to eliminate the term  $(\nabla\theta)^2$  from  $\Omega_{\text{kin}}^{(2)}$  when  $T \neq 0$ , so we must calculate it explicitly.

The  $O_1$  term in  $\Sigma$  yields

$$\Omega_{\text{kin}}^{(2)}(O_1) = \frac{T}{2} \int_0^\beta d\tau \int d\mathbf{r} \frac{T}{(2\pi)^2} \sum_{n=-\infty}^{\infty} \int d\mathbf{k} \text{Tr}[\mathcal{G}(i\omega_n, \mathbf{k})\tau_3\mathcal{G}(i\omega_n, \mathbf{k})\tau_3] \left( \frac{i\partial_\tau\theta}{2} + \frac{(\nabla\theta)^2}{8m} \right)^2. \quad (3.7)$$

Using (A.11) to compute the sum over the Matsubara frequencies, we find that

$$\Omega_{\text{kin}}^{(2)}(O_1) = -\frac{T}{2} \int_0^\beta d\tau \int d\mathbf{r} K(\mu, T, \rho) \left( i\partial_\tau\theta + \frac{(\nabla\theta)^2}{4m} \right)^2, \quad (3.8)$$

where

$$K(\mu, T, \rho(\mu, T)) = \frac{m}{8\pi} \left( 1 + \frac{\mu}{\sqrt{\mu^2 + \rho^2}} \tanh \frac{\sqrt{\mu^2 + \rho^2}}{2T} \right). \quad (3.9)$$

Obviously, the  $O_1$  term does not affect the coefficient of  $(\nabla\theta)^2$ . Further, it is easy to make sure that the cross term involving  $O_1$  and  $O_2$  in  $\Omega_{\text{kin}}^{(2)}$  is absent. Finally, calculations of the  $O_2$  contribution to  $\Omega_{\text{kin}}^{(2)}$  yield<sup>4</sup>

---

<sup>4</sup> Derivatives higher than  $(\nabla\theta)^2$  were not computed here.

$$\Omega_{\text{kin}}^{(2)}(O_2) = T \int_0^\beta d\tau \int d\mathbf{r} \frac{T}{(2\pi)^2} \sum_{n=-\infty}^{\infty} \int d\mathbf{k} \mathbf{k}^2 \text{Tr}[\mathcal{G}(i\omega_n, \mathbf{k}) \hat{I} \mathcal{G}(i\omega_n, \mathbf{k}) \hat{I}] \frac{(\nabla\theta)^2}{16m^2}. \quad (3.10)$$

Thus, summing over the Matsubara frequencies (see Eq. (A.12)), one obtains

$$\Omega_{\text{kin}}^{(2)}(O_2) = - \int_0^\beta d\tau \int d\mathbf{r} \frac{1}{128\pi^2 m^2} \int d\mathbf{k} \frac{\mathbf{k}^2}{\cosh^2 \frac{\sqrt{\xi^2(\mathbf{k}) + \rho^2}}{2T}} (\nabla\theta)^2. \quad (3.11)$$

As expected, this term vanishes when  $T \rightarrow 0$ , but at finite  $T$  it is comparable with (3.5).

Combining (3.5), (3.11), and (3.8) we finally obtain

$$\Omega_{\text{kin}} = \frac{T}{2} \int_0^\beta d\tau \int d\mathbf{r} \left[ n_F(\mu, T, \rho) i \partial_\tau \theta + J(\mu, T, \rho) (\nabla\theta)^2 + K(\mu, T, \rho) (\partial_\tau \theta)^2 \right], \quad (3.12)$$

where

$$J(\mu, T, \rho(\mu, T)) = \frac{1}{4m} n_F(\mu, T, \rho) - \frac{T}{4\pi} \int_{-\mu/2T}^{\infty} dx \frac{x + \mu/2T}{\cosh^2 \sqrt{x^2 + \frac{\rho^2}{4T^2}}} \quad (3.13)$$

characterizes the phase stiffness and governs the spatial variation of the phase  $\theta(\mathbf{r})$ . One can see that our value of the phase stiffness  $J(T=0)$  coincides with the nonrenormalized stiffness used in Ref. [27].

The quantity  $J(\mu, T, \rho)$  vanishes at  $\rho = 0$ , which means that above  $T_\rho$  the modulus-phase variables are meaningless; to study the model in this region one must use the old variables  $\Phi$  and  $\Phi^*$ . Near  $T_\rho$  one can obtain from (3.13) in the high-density limit (see below)

$$J(\mu \simeq \epsilon_F, T \rightarrow T_\rho, \rho \rightarrow 0) = \frac{7\zeta(3)}{16\pi^3} \frac{\rho^2}{T_\rho^2} \epsilon_F \simeq 0.016 \frac{\rho^2}{T_\rho^2} \epsilon_F. \quad (3.14)$$

Direct comparison of (3.12) with the Hamiltonian of the XY-model (3.1) makes it possible to write Eq. (3.2) for  $T_{\text{BKT}}$  directly:

$$\frac{\pi}{2} J(\mu, T_{\text{BKT}}, \rho(\mu, T_{\text{BKT}})) = T_{\text{BKT}}. \quad (3.15)$$

Although mathematically this reduces to a well-known problem, the analogy is incomplete. Indeed, in the standard XY-model (as well as the nonlinear  $\sigma$ -model) the vector (spin) subject to ordering is assumed to be a unit vector with no dependence on  $T$ .<sup>5</sup> In our case

---

<sup>5</sup> There is no doubt that in certain situations (for example, very high  $T$ ) it also can become a thermodynamic variable, i.e., one dependent on  $T$ , as happens in problems of phase transitions between ordered (magnetic) and disordered (paramagnetic) phases when the spin itself vanishes. Specifically, for quasi-2D spin systems it is obvious that as one proceeds from high- $T$  regions, a spin modulus first forms in 2D clusters of finite size and only then does global 3D ordering occur. We note, however, that this dependence was neglected in Ref. [27], where the nonrenormalized phase stiffness  $J(T=0)$  was used to write Eq. (3.15).

this is definitely not the case, and a self-consistent calculation of  $T_{\text{BKT}}$  as a function of  $n_f$  requires additional equations for  $\rho$  and  $\mu$ , which together with (3.15) form a complete set.

Using the definition (2.7), one can derive the effective potential  $\Omega_{\text{pot}}(v, \mu, T, \rho)$  (see Appendix A). Then the desired missing equations are the condition  $\partial\Omega_{\text{pot}}(\rho)/\partial\rho = 0$  that the potential (A.10) be minimized, and the equality  $v^{-1}\partial\Omega_{\text{pot}}/\partial\mu = -n_f$ , which fixes  $n_f$ . These are, respectively

$$\frac{1}{V} = \int \frac{d\mathbf{k}}{(2\pi)^2} \frac{1}{2\sqrt{\xi^2(\mathbf{k}) + \rho^2}} \tanh \frac{\sqrt{\xi^2(\mathbf{k}) + \rho^2}}{2T}, \quad (3.16)$$

$$n_F(\mu, T, \rho) = n_f, \quad (3.17)$$

where  $n_F(\mu, T, \rho)$  is defined by (3.6).

Equations (3.16) and (3.17) comprise a self-consistent system for determining the modulus  $\rho$  of the order parameter and the chemical potential  $\mu$  in the mean-field approximation for fixed  $T$  and  $n_f$ .

While Eqs. (3.16) and (3.17) seem to yield a reasonable approximation at high densities  $n_f$ , since they include condensed boson pairs in a nonperturbative way via nonzero  $\rho$ , they must certainly be corrected in the strong coupling regime (low densities  $n_f$ ) to take into account the contribution of noncondensed bosons (this appears to be important also for Eq. (3.15), which determines  $T_{\text{BKT}}$ ). The extent to which this alters the present results is not completely clear. Previously, the best way to incorporate noncondensed pairs seems to have been the self-consistent  $T$ -matrix approximation [10,30–32], which allows one to account for the feedback of pairs on the self-energy of fermions. However, the  $T$ -matrix approach, at least in its standard form [10,30–32], fails to describe the BKT phase transition, for which one must consider the equation for the vertex. On the other hand, in our approach the BKT phase transition is realized by the condition (3.2), while an analog of the  $T$ -matrix approximation in terms of propagators of the  $\rho$ -particle and the neutral fermion  $\chi$  has yet to be elaborated.

The energy of two-particle bound states in a vacuum

$$\varepsilon_b = -2W \exp\left(-\frac{4\pi}{mV}\right) \quad (3.18)$$

(see Refs. [4,7] and [33]) is more convenient to use than the four-fermion constant  $V$  (here  $W$  is the conduction bandwidth). For example, one can easily take the limits  $W \rightarrow \infty$  and  $V \rightarrow 0$  in Eq. (3.16), which after this renormalization becomes

$$\ln \frac{|\varepsilon_b|}{\sqrt{\mu^2 + \rho^2} - \mu} = 2 \int_{-\mu/T}^{\infty} du \frac{1}{\sqrt{u^2 + \left(\frac{\rho}{T}\right)^2} \left[ \exp \sqrt{u^2 + \left(\frac{\rho}{T}\right)^2} + 1 \right]}. \quad (3.19)$$

Thus, in practice, we solve Eqs. (3.15), (3.17), and (3.19) numerically to study  $T_{\text{BKT}}$  as function of  $n_f$  (or equivalently, of the Fermi energy  $\epsilon_F = \pi n_f/m$ , as it should be for 2D metals with the simplest quadratic dispersion law).



It is easy to show that at  $T = 0$ , the system (3.17), (3.19) transforms into a previously studied system (see Ref. [4] and references therein). Its solution is  $\rho = \sqrt{2|\varepsilon_b|\epsilon_F}$  and  $\mu = -|\varepsilon_b|/2 + \epsilon_F$ . This will be useful in studying the concentration dependencies of  $2\Delta/T_{\text{BKT}}$  and  $2\Delta/T_\rho$ , where  $\Delta$  is the zero-temperature gap in the quasiparticle excitation spectrum. It should be borne in mind that in the local pair regime ( $\mu < 0$ ), the gap  $\Delta$  equals  $\sqrt{\mu^2 + \rho^2}$  rather than  $\rho$  (as in the case  $\mu > 0$ ) [4].

Setting  $\rho = 0$  in Eqs. (3.16) and (3.17), we obtain (in the same approximation) the equations for the critical temperature  $T_\rho$  and the corresponding value of  $\mu$ :

$$\ln \frac{|\varepsilon_b|}{T_\rho} \frac{\gamma}{\pi} = - \int_0^{\mu/2T_\rho} du \frac{\tanh u}{u} \quad (\gamma = 1.781), \quad (3.20)$$

$$T_\rho \ln \left[ 1 + \exp \left( \frac{\mu}{T_\rho} \right) \right] = \epsilon_F. \quad (3.21)$$

Note that these equations coincide with the system that determines the mean-field temperature  $T_c^{(2D)MF} (= T_\rho)$  and  $\mu(T_c^{(2D)MF})$  [7], evidently as a result of the mean-field approximation for the variable  $\rho$  used here. There is, however, an important difference between the temperatures  $T_c^{2D}$  and  $T_\rho$ . Specifically, if one takes fluctuations into account,  $T_c^{2D}$  goes to zero, while the value of  $T_\rho$  remains finite. The crucial point is that the perturbation theory in the variables  $\rho$  and  $\theta$  does not contain any infrared singularities [22,34], in contrast to the perturbation theory in  $\Phi, \Phi^*$ ; thus the fluctuations do not reduce  $T_\rho$  to zero. This is why the temperature  $T_\rho$  has its own physical meaning: incoherent (local or Cooper) pairs begin to form (at least at high enough  $n_f$  (see Sec. V)) just below  $T_\rho$ . At higher temperatures, only these pair fluctuations exist; their influence was studied in Ref. [35].

#### IV. NUMERICAL RESULTS

A numerical investigation of the systems (3.15), (3.17), (3.19), and (3.20), (3.21) yields the following results, which are displayed graphically as the phase diagram of the system.

a) For low carrier densities, the pseudogap phase area (see Fig. 1) is comparable with the BKT area. For high carrier densities ( $\epsilon_F \gtrsim 10^3 |\varepsilon_b|$ ), one easily finds that the pseudogap region shrinks asymptotically as

$$\frac{T_\rho - T_{\text{BKT}}}{T_\rho} \simeq \frac{4T_\rho}{\epsilon_F}. \quad (4.1)$$

This behavior qualitatively restores the BCS limit observed in overdoped samples.

b) For  $\epsilon_F \leq (10 - 15)|\varepsilon_b|$ , the function  $T_{\text{BKT}}(\epsilon_F)$  is linear, as also confirmed by the analytic solution of the system (3.15), (3.17), and (3.19), which yields  $T_{\text{BKT}} = \epsilon_F/8$ . Remarkably, such behavior of  $T_c(\epsilon_F)$  is observed for all families of HTSC cuprates in their underdoped region [3,27], though with a smaller coefficient of proportionality (0.01 – 0.1). This indicates the importance of including a contribution due to noncondensed pairs in Eq. (3.15), which defines  $T_{\text{BKT}}$ .

It has been shown that for optimal doping, the dimensionless ratio  $\epsilon_F/|\varepsilon_b| \sim 3 \cdot 10^2 - 10^3$  [36]. Thus it is quite natural to suppose that in the underdoped region one has  $\epsilon_F/|\varepsilon_b| \sim 10 - 10^2$ , where we find linear behavior.

We note that in this limit, the temperature  $T_c$  of formation of a homogeneous order parameter for the quasi-2D model [3,6] can easily be written in the form

$$T_c \approx \frac{4T_{\text{BKT}}}{\ln(\epsilon_F|\varepsilon_b|/4t_{\parallel}^2)}, \quad (4.2)$$

where  $t_{\parallel}$  is the interplane hopping (coherent tunneling) constant. This shows that when  $T_c < T_{\text{BKT}}$ , the weak three-dimensionalization can preserve (in any case, at low  $n_f$ ) the regions of the pseudogap and BKT phases, which, for example, happens in the relativistic quasi-2D model [34]. At the same time, as the three-dimensionalization parameter  $t_{\parallel}$  increases, when  $T_c > T_{\text{BKT}}$  the BKT phase can vanish, provided, however, that the anomalous phase region and both temperatures  $T_{\rho}$  and  $T_c \simeq n_f/m$  are preserved.

c) Figure 2 shows the values of  $n_f$  for which  $\mu$  differs substantially from  $\epsilon_F$ , or in other words, the Landau Fermi-liquid theory becomes inapplicable to metals (also called bad ones) with low or intermediate carrier density. As expected, the kink  $\mu$  at  $T = T_{\rho}$ , which has been observed experimentally [37] and interpreted for the 1-2-3 cuprates [38], becomes less and less pronounced as  $\epsilon_F$  increases. But in the present case it is interesting that in the hydrodynamic approximation employed here, it happens at the normal-pseudogap phase boundary or before superconductivity really appears. It would therefore be of great interest to perform experiments that might reveal the temperature dependence  $\mu(T)$ , especially for strongly anisotropic and relatively weakly doped cuprates.

d) It follows from curve 3 in Fig. 2 that the crossover (sign change in  $\mu$ ) from local to Cooper pairs is possible not only as  $\epsilon_F$  increases, which is more or less obvious, but also (for some  $n_f$ ) as  $T$  increases.

e) Finally the calculations showed (see Fig. 3) that the ratio  $2\Delta/T_{\text{BKT}}$  is greater than 4.7 in the region under study. The value  $2\Delta/T_{\rho}(= 2\Delta/T_c^{MF})$  is, however, somewhat lower and reaches the BCS theory limit of 3.52 only for  $\epsilon_F \gg |\varepsilon_b|$ . It is interesting that this concentration behavior is consistent with numerous measurements of this ratio in HTSC [39,40]. Note that the divergence of  $2\Delta/T_{\text{BKT}}$  and  $2\Delta/T_{\rho}$  at  $\epsilon_F \rightarrow 0$  is directly related to the definition of  $\Delta$  at  $\mu < 0$ .

## V. PAIRING TEMPERATURE $T_P$ VERSUS CARRIER DENSITY

There is no disagreement concerning the asymptotic behavior of  $T_{\text{BKT}}$  (or  $T_c$ )  $\sim \epsilon_F$  in the region of low carrier densities. In contrast, the behavior of the temperature  $T_{\rho}$ , below which pairs are formed, cannot be considered to be generally accepted. For example, in Refs. [3] and [27], based on qualitative arguments, this temperature is taken to be the temperature  $T_P$  of local uncorrelated pairing, which in contrast to  $T_{\rho}$  increases with decreasing  $n_f$ .<sup>6</sup>

---

<sup>6</sup>In fact, in Refs. [3] and [27] (see also Ref. [5]) this temperature was plotted as an increasing function of coupling constant  $V$ , which for 3D systems corresponds, to some extent, to the carrier

Randeria (see Ref. [4] and references therein), to define the pairing temperature  $T_P$ , uses the system of equations for the mean-field transition temperature and the corresponding chemical potential, which is essentially identical to the system (3.20), (3.21). Thus his  $T_P \rightarrow 0$  as  $n_f \rightarrow 0$ .

It is also well known [4,5,9] that in the low-density limit, it is vital to include quantum fluctuations, at least in the number equation [12], in the calculation of the critical temperature at which long-range order forms in 3D. In 2D these fluctuations in fact reduce the critical temperature to zero [11]. Certainly quantum fluctuations are also important in the calculation of  $T_\rho$  in the limit  $n_f \rightarrow 0$  and, in particular, in the number equation. However, as already stressed in Sec. III, these corrections are quite different from what we obtain using the variables  $\Phi, \Phi^*$ , since perturbation theory in the variables  $\rho$  and  $\theta$  does not contain any infrared singularities [22,34], and the fluctuations do not yield  $T_\rho \equiv 0$ . In fact, even including quantum fluctuations,  $T_\rho$  must exceed  $T_{\text{BKT}}$  ( $\rho(T_{\text{BKT}}) \neq 0$ ), so that the pseudogap phase is always present.

In our opinion, the temperature  $T_\rho$  has its own physical interpretation: this is the temperature of a smooth transition to the state in which the neutral order parameter  $\rho \neq 0$ , and below which one can observe pseudogap manifestations. There is also a very interesting and important question about the character of the transition. Certainly in the simplest Landau theory one appears to have a second-order phase transition, since  $\rho$  takes a nonzero value only below  $T_\rho$  [14]. However this kind of transition is only possible for neutral fermions. Fluctuations of the  $\theta$ -phase will transform the pole in the Green function of the neutral fermions into a branch cut in the Green function for charged particles in the BKT phase. Indeed, the CMWH theorem concerning the absence of spontaneous breaking of a continuous symmetry means that symmetry-violating Green functions must vanish. However, it says nothing about the gap in the spectrum of excitations, as is sometimes incorrectly stated.

The correct explanation is that if the symmetry is unbroken, *and* the fermion excitation appears as a pole in the  $\psi$  two-point function, then the fermion must be gapless. If the fermion does not have the same quantum numbers as  $\psi$  (like our fermion  $\chi$ ) and so does not appear in the  $\psi$  two-point function as a one-particle state, then the symmetry does not tell whether the fermion ( $\chi$ ) will be gapless or not.

This very general argument [22] suggests the following plausible scenario. At low temperatures ( $T < T_{\text{BKT}}$ ),  $\chi, \rho$ , and  $\theta$  should be treated as physical quasiparticles ( $\chi, \rho$  having a gap and  $\theta$  being a gapless excitation), while a straightforward computation of the  $\psi$  two-point function [22] reveals its branch-cut structure.

On the other hand, at temperatures above  $T_{\text{BKT}}$ , we should consider  $\psi$  and  $\Phi$  true quasiparticles, since  $T_{\text{BKT}}$  is a phase transition point and the spectrum of physical excitations changes precisely at this point. The  $\psi$  two-point function at  $T > T_{\text{BKT}}$  should be studied separately due to the presense of vortices which change the form of the correlator  $\langle \exp[i\theta(x)] \exp[i\theta(0)] \rangle$  above  $T_{\text{BKT}}$ . In this temperature region the  $\psi$  two-point function loses its branch-cut structure; instead, it acquires the form suggested in Refs. [30] and [31]

---

density decreasing. In 2D systems, however, where, as is well known, two-particle bound states are formed without any threshold, similar conclusions about the behavior of  $T_P(n_f)$  are questionable, and must be checked independently.

with a pseudogap originating from the superconducting gap below  $T_{\text{BKT}}$ , which preserves “BCS-like” structure as well as the diagonal component of the single-particle Green function. In this picture the Fermi-liquid description breaks down, evidently below  $T_\rho$ , due to the formation of nonzero  $\rho$ .

We note, however, that the decisive confirmation of this picture demands further detailed study probably based on a different approach, for example the self-consistent  $T$ -matrix (see Ref. [30] and references therein), which enables one to directly obtain the full fermion Green function.

To define the temperature  $T_P$  properly, one should study the spectrum of bound states either by solving the Bethe–Salpeter equation [7] or by analyzing the corresponding Green functions as we do here. It turns out that there is no difference between  $T_P$  and  $T_\rho$  in the Cooper pair regime ( $\mu > 0$ ), while in the local pair region ( $\mu < 0$ ) these temperatures exhibit different behavior.

Indeed, let us study the spectrum of bound states in both the normal ( $\rho = 0$ ) and pseudogap ( $\rho \neq 0$ ) phases. We are especially interested in determining the conditions under which real bound states (with zero total momentum  $\mathbf{K} = 0$ ) become unstable. For this purpose one can look at the propagator of the  $\rho$ -particle in the pseudogap phase:

$$\Gamma^{-1}(\tau, \mathbf{r}) = \frac{1}{2} \frac{\beta \delta^2 \Omega(v, \mu, T, \rho(\tau, \mathbf{r}), \partial \theta(\tau, \mathbf{r}))}{\delta \rho(\tau, \mathbf{r}) \delta \rho(0, 0)} \Big|_{\rho=\rho_{\min}=\text{const}}, \quad (5.1)$$

where  $\rho_{\min}$  is defined by the minimum condition (3.16) (or (3.19)) of the potential part (A.10) of the effective action (2.3). In the momentum representation, the spectrum of bound states is usually determined by the condition

$$\Gamma_R^{-1}(\omega, \mathbf{K}) = 0, \quad (5.2)$$

where  $\Gamma_R(\omega, \mathbf{K})$  is the retarded Green function obtained directly from the temperature Green function  $\Gamma(i\Omega_n, \mathbf{K})$  using the analytic continuation  $i\Omega_n \rightarrow \omega + i0$ . Recall that such analytic continuation must be performed after evaluating the sum over the Matsubara frequencies. In the case of vanishing total momentum  $\mathbf{K} = 0$ , one arrives at the energy spectrum equation

$$\Gamma_R^{-1}(\omega, 0) = \frac{1}{V} + 2 \int \frac{d\mathbf{k}}{(2\pi)^2} \frac{\xi^2(\mathbf{k})}{\sqrt{\xi^2(\mathbf{k}) + \rho^2}} \frac{\tanh \sqrt{\xi^2(\mathbf{k}) + \rho^2}/2T}{\omega^2 - 4[\xi^2(\mathbf{k}) + \rho^2]} = 0. \quad (5.3)$$

From the explicit expression (5.3) for  $\Gamma_R(\omega, 0)$ , this function obviously has a branch cut at frequencies

$$|\omega| \geq 2 \min \sqrt{\xi^2(\mathbf{k}) + \rho^2} = \begin{cases} 2\rho, & \mu \geq 0 \\ 2\sqrt{\mu^2 + \rho^2}, & \mu < 0. \end{cases} \quad (5.4)$$

Thus, bound states can exist below this cut.

Real bound states decay into two-fermion states when the energy of the former reaches the branch point  $2 \min \sqrt{\xi^2(\mathbf{k}) + \rho^2}$ . Since  $\Gamma_R^{-1}$  is a monotonically decreasing function of  $\omega^2$ , it has the unique solution  $|\varepsilon_b(T)| = 2\rho(T)$ , at which Eq. (5.3) coincides exactly with the mean-field equation (3.16) for  $\rho(T)$ . It also becomes clear that for  $\mu < 0$  we have real bound

states with energy  $\varepsilon_b(T)$  below the two-particle scattering continuum at  $\omega = 2\sqrt{\mu^2 + \rho^2}$ , while at  $\mu \geq 0$  there are no stable bound states. The line  $\mu(T, \epsilon_F) = 0$  in the  $T$ - $\epsilon_F$  plane at  $\rho \neq 0$  separates the negative  $\mu$  region where local pairs exist from that in which only Cooper pairs exist (positive  $\mu$ ). This line (see Fig. 4) begins at the point  $T = (e^\gamma/\pi)|\varepsilon_b| \approx 0.6|\varepsilon_b|$ ,  $\epsilon_F \approx 0.39|\varepsilon_b|$  and ends at  $T = 0$ ,  $\epsilon_F = |\varepsilon_b|/2$ . (The latter follows directly from the solution at  $T = 0$ ,  $\mu = -|\varepsilon_b|/2 + \epsilon_F$  [4,7].)

To find a similar line in the normal phase with  $\rho = 0$ , we consider the corresponding equation for the bound states. The propagator of these states (in imaginary time formalism) is defined to be

$$\Gamma^{-1}(\tau, \mathbf{r}) = \frac{\beta \delta^2 \Omega(v, \mu, T, \Phi(\tau, \mathbf{r}), \Phi^*(\tau, \mathbf{r}))}{\delta \Phi^*(\tau, \mathbf{r}) \delta \Phi(0, 0)} \Big|_{\Phi=\Phi^*=0}. \quad (5.5)$$

(In the normal phase, where  $\rho = 0$ , we must again use the initial auxiliary fields  $\Phi$  and  $\Phi^*$  (see Secs. II. and III).) Then in the momentum representation (after summing over the Matsubara frequencies) we have

$$\Gamma^{-1}(i\Omega_n, \mathbf{K}) = \frac{1}{V} - \frac{1}{2} \int \frac{d\mathbf{k}}{(2\pi)^2} \frac{\tanh \xi_+(\mathbf{k}, \mathbf{K})/2T + \tanh \xi_-(\mathbf{k}, \mathbf{K})/2T}{\xi_+(\mathbf{k}, \mathbf{K}) + \xi_-(\mathbf{k}, \mathbf{K}) - i\Omega_n},$$

$$\xi_{\pm}(\mathbf{k}, \mathbf{K}) \equiv \frac{1}{2m} \left( \mathbf{k} \pm \frac{\mathbf{K}}{2} \right)^2 - \mu, \quad (5.6)$$

where  $\mathbf{k}$  is the relative momentum of the pair. The spectrum of bound states is given again by Eq. (5.2). Using the energy  $\varepsilon_b$  (see Eq. (3.18)) of the bound state at  $T = 0$ , for  $\mathbf{K} = 0$  we obtain the following equation for the energies of these states in the normal phase:

$$\int_0^\infty dx \left[ \frac{1}{x + |\varepsilon_b|/2} - \frac{\tanh(x - \mu)/2T}{x - \mu - \omega/2} \right] = 0. \quad (5.7)$$

Such states can exist provided  $-2\mu - |\varepsilon_b| < \omega < -2\mu$ . The left-hand side of Eq. (5.7) is positive at  $\omega = -2\mu - |\varepsilon_b|$  and tends to  $+\infty$  ( $\mu > 0$ ) or  $-\infty$  ( $\mu < 0$ ) when  $\omega \rightarrow -2\mu$ . This equation always has a solution at  $\mu < 0$ , so bound states with zero total momentum exist for negative  $\mu$ .

For  $\mu > 0$ , analytic analysis becomes more complicated, and requires numerical study. One can easily find from (5.7) that at  $T = 0$ , stable bound states exist up to  $\mu < |\varepsilon_b|/8$ . In fact, numerical study for  $T \geq T_\rho$  shows that the trajectory  $\mu(T, \epsilon_F) = 0$  (or  $T = \epsilon_F/\ln 2$ , see (3.21)) approximately divides the normal phase into two qualitatively different regions – with ( $\mu < 0$ ) and without ( $\mu > 0$ ) stable (long-lived) pairs. This also holds for other phases, which enables one to draw the whole line  $\mu(T, \epsilon_F) = 0$  (Fig. 4).

Knowing the two-particle binding energy, it is natural to define pairing temperature  $T_P$  as  $T_P \approx |\varepsilon_b(T_P, \mu(T_P, \epsilon_F))|$ . This equation can be easily analyzed in the region  $\epsilon_F \ll |\varepsilon_b|$ , for which we directly obtain  $T_P \approx |\varepsilon_b|$ , which clearly coincides with the standard estimate [3,41]. This means in turn that the curve  $T_P(\epsilon_F)$  starting at  $T_P(0) \approx |\varepsilon_b|$  will be reduced, up to the point  $T_P(0.39\epsilon_F) \approx 0.6|\varepsilon_b|$ , which lies on the line  $T_\rho(\epsilon_F)$  (see Fig. 4). It is important that this line is not the phase transition curve; it merely divides the fermion system diagram into temperature regions with a prevailing mean number of local pairs ( $T \lesssim T_P$ ) or unbound carriers ( $T \gtrsim T_P$ ). This is the region of the abnormal normal phase where one has preformed

boson pairs. It is widely accepted, however, that this case is only of theoretical interest, since there is no Fermi surface ( $\mu < 0$ ) in the phase. The phase area or the difference  $T_P(\epsilon_F) - T_\rho(\epsilon_F)$  is an increasing function as  $\epsilon_F \rightarrow 0$ , which corresponds to the behavior usually assumed [3,27].

When  $\mu > 0$  there are no stable bound states ( $\varepsilon_b(T) = 2\rho(T) = 0$ ) for the normal phase, where they are short-lived. Formally, using  $\rho(T) = 0$  in Eq. (5.3), we immediately obtain (3.20) or, in other words, here  $T_P = T_\rho$ . Such a conclusion is in accordance with the generally accepted definition of  $T_P$  in the BCS case [41].

Thus the phase diagram of a 2D metal above  $T_c$  acquires the form shown in Fig. 4. It is interesting that if the line  $T_P(\epsilon_F)$  cannot be defined exactly, the temperature  $T_\rho(\epsilon_F)$  is the line below which pairs reveal some signs of collective behavior. Moreover, at  $T < T_\rho$  one can speak of a real pseudogap in the one-particle spectrum, while in the region  $T_\rho < T < T_P$  only strongly developed pair fluctuations (some number of pairs) exist, though they probably suffice to reduce the spectral quasi-particle weight, and to produce other observed manifestations that mask pseudogap (spin gap; see Ref. [35]) formation.

## VI. PARAMAGNETIC SUSCEPTIBILITY OF THE SYSTEM

It would be very interesting to study how a nonzero value of the neutral order parameter affects the observable properties of the 2D system. Does this really resemble the gap opening in the traditional superconductors, except that it happens in the normal phase? Or, in other words, does the pseudogap open?

We shall demonstrate this phenomenon, taking the paramagnetic susceptibility of the system as the simplest case in point. To study the system in the magnetic field  $\mathbf{H}$  one must add the paramagnetic term

$$\mathcal{H}_{PM} = -\mu_B H [\psi_\uparrow^\dagger(\mathbf{r})\psi_\uparrow(\mathbf{r}) - \psi_\downarrow^\dagger(\mathbf{r})\psi_\downarrow(\mathbf{r})] \quad (6.1)$$

to the Hamiltonian (2.1) where  $\mu_B = e\hbar/2mc$  is the Bohr magneton. Note that, using the isotropy in the problem, we chose the direction of field  $\mathbf{H}$  to be perpendicular to the plane containing the vectors  $\mathbf{r}$ .

Adding the corresponding term to Eq. (2.8) for the neutral fermion Green function, it is easy to show that in the momentum representation (compare with (3.4))

$$\mathcal{G}(i\omega_n, \mathbf{k}, H) = \frac{(i\omega_n + \mu_B H)\hat{I} + \tau_3 \xi(\mathbf{k}) - \tau_1 \rho}{(i\omega_n + \mu_B H)^2 - \xi^2(\mathbf{k}) - \rho^2}. \quad (6.2)$$

The static paramagnetic susceptibility can be expressed in terms of the magnetization,

$$\chi(\mu, T, \rho) = \left. \frac{\partial M(\mu, T, \rho, H)}{\partial H} \right|_{H=0}, \quad (6.3)$$

which in the mean-field approximation can be derived from the effective potential:

$$M(\mu, T, \rho, H) = -\frac{1}{v} \frac{\partial \Omega_{\text{pot}}(v, \mu, T, \rho, H)}{\partial H}. \quad (6.4)$$

Thus from (6.4) one obtains

$$M(\mu, T, \rho, H) = \mu_B T \sum_{n=-\infty}^{\infty} \int \frac{d\mathbf{k}}{(2\pi)^2} \text{Tr}[\mathcal{G}(i\omega_n, \mathbf{k}, H) \hat{I}]. \quad (6.5)$$

Then using the definition (6.3) one arrives at

$$\chi(\mu, T, \rho) = \mu_B^2 \int \frac{d\mathbf{k}}{(2\pi)^2} 2T \sum_{n=-\infty}^{\infty} \frac{\xi^2(\mathbf{k}) + \rho^2 - \omega_n^2}{[\omega_n^2 + \xi^2(\mathbf{k}) + \rho^2]^2}. \quad (6.6)$$

The sum in (6.6) can easily be calculated with the help of Eq. (A.11); thus, we obtain the final result

$$\chi(\mu, T, \rho) = \chi_{\text{Pauli}} \frac{1}{2} \int_{-\mu/2T}^{\infty} \frac{dx}{\cosh^2 \sqrt{x^2 + \frac{\rho^2}{4T^2}}}, \quad (6.7)$$

where  $\chi_{\text{Pauli}} \equiv \mu_B^2 m / \pi$  is the Pauli paramagnetic susceptibility for the 2D system.

To study  $\chi$  as a function of  $T$  and  $n_f$  (or  $\epsilon_F$ ), Eq. (6.7) should be used together with Eqs. (3.17) and (3.19).

For the case of the normal phase ( $\rho = 0$ ) one can investigate the system analytically. Thus (6.7) takes the form

$$\chi(\mu, T, \rho = 0) = \chi_{\text{Pauli}} \frac{1}{1 + \exp(-\mu/T)}, \quad (6.8)$$

where  $\mu$  is determined by (3.21). This system has the solution

$$\chi(\epsilon_F, T, \rho = 0) = \chi_{\text{Pauli}} [1 - \exp(-\epsilon_F/T)], \quad (6.9)$$

which is identical to a solution known from the literature [42].

The results of a numerical study of the system (6.7), (3.19), and (3.17) are presented in Fig. 5. One can see that the kink in  $\chi$  occurs at  $T = T_\rho$  as in the dependence of  $\mu$  on  $T$ . Below  $T_\rho$  the value of  $\chi(T)$  decreases, although the system is still normal. This can be interpreted as a spin-gap (or pseudogap) opening. The size of the pseudogap region depends strongly on the doping ( $\epsilon_F/|\varepsilon_b|$ ), as observed for real HTSC [2,18,19]. For small values of  $\epsilon_F/|\varepsilon_b|$  this region is very large ( $T_\rho > 6T_{\text{BKT}}$ ), while for large  $\epsilon_F/|\varepsilon_b| \sim 5 - 30$  it is slightly larger than the region corresponding to the BKT phase.

## VII. CONCLUSION

To summarize, we have discussed the crossover in the superconducting transition between BCS- and Bose-like behavior for the simplest 2D model, with s-wave nonretarded attractive interaction.

While there is still no generally accepted microscopic theory of HTSC compounds and their basic features (including the pairing mechanism), it seems that this approach, although in a sense phenomenological, is of great interest since it is able to cover the whole range of

carrier concentrations (and thus the whole range of coupling constants) and temperatures. As we tried to demonstrate, it enables one to propose both a reasonable interpretation for the observed phenomena caused by doping and to describe new phenomena—for example, pseudogap phase formation as a new thermodynamically equilibrium normal state of low-dimensional conducting electronic systems.

Evidently there are a number of important open questions. They may be divided into two classes: the first concerns the problem of a better and more complete treatment of the models themselves. The second class relates to the extent to which this model is applicable to HTSC compounds, and what the necessary ingredients are for a more realistic description.

Regarding the microscopic Hamiltonian as a given model, our treatment is obviously still incomplete. In particular, there exists an unconfirmed numerical result [43] based on a fully self-consistent determination of a phase transition to a superconducting state in a conserving approximation, which states that the superconducting transition is neither the simple mean-field transition nor the BKT transition. (See, however, the discussion preceding Eq. (3.18).) Besides, it would be very interesting to obtain the spectrum of both the anomalous normal and pseudogap phases. It is important also to take into consideration the effects of noncondensed bosons, which might help to obtain a smaller slope in the dependence of  $T_{\text{BKT}}$  on  $\epsilon_F$ .

As for the extent to which the models considered are really applicable to HTSC, most of the complexity of these systems is obviously neglected here. For example, we did not take into account the indirect nature of attraction between the fermions,  $d$ -wave pairing, inter-layer tunneling, etc. Nevertheless, one may hope that the present simple model can explain the essential features of pseudogap formation.

## ACKNOWLEDGMENTS

We thank Drs. E. V. Gorbar, I. A. Shovkovy, O. Tchernyshyov, and V. M. Turkowski for fruitful discussions, which helped to clarify some deep questions about low-dimensional phase transitions. We especially thank Prof. R. M. Quick for many thoughtful comments on an earlier version of this manuscript. One of us (S. G. S) is grateful to the members of the Department of Physics of the University of Pretoria, especially Prof. R. M. Quick and Dr. N. J. Davidson, for very useful points and hospitality. S.G.S also acknowledges the financial support of the Foundation for Research Development, Pretoria.

## APPENDIX A: CALCULATION OF THE EFFECTIVE POTENTIAL

Here we sketch the derivation of the effective potential. To obtain it one must write Eq. (2.7) in the momentum representation:

$$\begin{aligned} \Omega_{\text{pot}}(v, \mu, T, \rho) = & v \left\{ \frac{\rho^2}{V} - T \sum_{n=-\infty}^{+\infty} \int \frac{d\mathbf{k}}{(2\pi)^2} \text{Tr}[\ln \mathcal{G}^{-1}(i\omega_n, \mathbf{k}) e^{i\delta\omega_n\tau_3}] \right. \\ & \left. + T \sum_{n=-\infty}^{+\infty} \int \frac{d\mathbf{k}}{(2\pi)^2} \text{Tr}[\ln G_0^{-1}(i\omega_n, \mathbf{k}) e^{i\delta\omega_n\tau_3}] \right\}, \quad \delta \rightarrow +0, \end{aligned} \quad (\text{A.1})$$



where

$$\mathcal{G}^{-1}(i\omega_n, \mathbf{k}) = i\omega_n \hat{I} - \tau_3 \xi(\mathbf{k}) + \tau_1 \rho, \quad G_0^{-1}(i\omega_n, \mathbf{k}) = \mathcal{G}^{-1}(i\omega_n, \mathbf{k}) \Big|_{\rho=\mu=0} \quad (\text{A.2})$$

are the inverse Green functions. The exponential factor  $e^{i\delta\omega_n\tau_3}$  is added to (A.1) to provide the correct regularization which is necessary to perform the calculation with the Green functions [44]. For instance, one obtains

$$\begin{aligned} \lim_{\delta \rightarrow +0} \sum_{n=-\infty}^{+\infty} \text{Tr}[\ln \mathcal{G}^{-1}(i\omega_n, \mathbf{k}) e^{i\delta\omega_n\tau_3}] &= \lim_{\delta \rightarrow +0} \left\{ \sum_{n=-\infty}^{+\infty} \text{Tr}[\ln \mathcal{G}^{-1}(i\omega_n, \mathbf{k})] \cos \delta\omega_n + \right. \\ &\quad \left. i \sum_{\omega_n > 0} \sin \delta\omega_n \text{Tr}[(\ln \mathcal{G}^{-1}(i\omega_n, \mathbf{k}) - \ln \mathcal{G}^{-1}(-i\omega_n, \mathbf{k}))\tau_3] \right\} \\ &= \sum_{n=-\infty}^{+\infty} \text{Tr}[\ln \mathcal{G}^{-1}(i\omega_n, \mathbf{k})] - \frac{\xi(\mathbf{k})}{T}, \end{aligned} \quad (\text{A.3})$$

where

$$\ln \frac{\mathcal{G}^{-1}(i\omega_n, \mathbf{k})}{i\omega_n} \simeq \frac{-\tau_3 \xi(\mathbf{k}) + \tau_1 \rho}{i\omega_n}, \quad \omega_n \rightarrow \infty$$

and

$$\sum_{\omega_n > 0} \frac{\sin \delta\omega_n}{\omega_n} \simeq \frac{1}{2\pi T} \int_0^\infty dx \frac{\sin \delta x}{x} = \frac{1}{4T} \text{sign } \delta.$$

To calculate the sum in (A.3), one must first use the identity  $\text{Tr} \ln \hat{A} = \ln \det \hat{A}$ , so that (A.1) takes the form

$$\Omega_{\text{pot}}(v, \mu, T, \rho) = v \left\{ \frac{\rho^2}{V} - T \sum_{n=-\infty}^{+\infty} \int \frac{d\mathbf{k}}{(2\pi)^2} \ln \frac{\det \mathcal{G}^{-1}(i\omega_n, \mathbf{k})}{\det G_0^{-1}(i\omega_n, \mathbf{k})} - \int \frac{d\mathbf{k}}{(2\pi)^2} [-\xi(\mathbf{k}) + \varepsilon(\mathbf{k})] \right\}. \quad (\text{A.4})$$

Calculating the determinants of the Green functions (A.2) one obtains

$$\Omega_{\text{pot}}(v, \mu, T, \rho) = v \left\{ \frac{\rho^2}{V} - T \sum_{n=-\infty}^{+\infty} \int \frac{d\mathbf{k}}{(2\pi)^2} \ln \frac{\omega_n^2 + \xi^2(\mathbf{k}) + \rho^2}{\omega_n^2 + \varepsilon^2(\mathbf{k})} - \int \frac{d\mathbf{k}}{(2\pi)^2} [-\xi(\mathbf{k}) + \varepsilon(\mathbf{k})] \right\}, \quad (\text{A.5})$$

where the role of  $G_0(i\omega_n, \mathbf{k})$  in the regularization of  $\Omega_{\text{pot}}$  is now evident. The summation in (A.5) can be done if one uses the representation

$$\ln \frac{\omega_n^2 + a^2}{\omega_n^2 + b^2} = \int_0^\infty dx \left( \frac{1}{\omega_n^2 + a^2 + x} - \frac{1}{\omega_n^2 + b^2 + x} \right), \quad (\text{A.6})$$

and then

$$\sum_{k=0}^{\infty} \frac{1}{(2k+1)^2 + c^2} = \frac{\pi}{4c} \tanh \frac{\pi c}{2}. \quad (\text{A.7})$$

We find

$$\ln \frac{\omega_n^2 + a^2}{\omega_n^2 + b^2} = \int_0^{\infty} dx \left( \frac{1}{2\sqrt{b^2 + x}} \tanh \frac{\sqrt{b^2 + x}}{2T} - \frac{1}{2\sqrt{a^2 + x}} \tanh \frac{\sqrt{a^2 + x}}{2T} \right). \quad (\text{A.8})$$

Integrating (A.8) over  $x$ , one thus obtains

$$T \sum_{n=-\infty}^{+\infty} \int \frac{d\mathbf{k}}{(2\pi)^2} \ln \frac{\omega_n^2 + \xi^2(\mathbf{k}) + \rho^2}{\omega_n^2 + \varepsilon^2(\mathbf{k})} = 2T \int \frac{d\mathbf{k}}{(2\pi)^2} \ln \frac{\cosh[\sqrt{\xi^2(\mathbf{k}) + \rho^2}/2T]}{\cosh[\varepsilon(\mathbf{k})/2T]}. \quad (\text{A.9})$$

Finally, substituting (A.9) into (A.5),

$$\Omega_{\text{pot}}(v, \mu, T, \rho) = v \left\{ \frac{\rho^2}{V} - \int \frac{d\mathbf{k}}{(2\pi)^2} \left[ 2T \ln \frac{\cosh[\sqrt{\xi^2(\mathbf{k}) + \rho^2}/2T]}{\cosh[\varepsilon(\mathbf{k})/2T]} - [\xi(\mathbf{k}) - \varepsilon(\mathbf{k})] \right] \right\}. \quad (\text{A.10})$$

It is easy to show that at  $T = 0$ , the expression (A.10) reduces to that obtained in Ref. [7].

Finally, we give formulas for the summation over the Matsubara frequencies used in Secs. III and VI:

$$\begin{aligned} T \sum_{n=-\infty}^{\infty} \text{Tr}[\mathcal{G}(i\omega_n, \mathbf{k}) \tau_3 \mathcal{G}(i\omega_n, \mathbf{k}) \tau_3] &= 2T \sum_{n=-\infty}^{\infty} \frac{\xi^2(\mathbf{k}) - \rho^2 - \omega_n^2}{[\omega_n^2 + \xi^2(\mathbf{k}) + \rho^2]^2} \\ &= -\frac{\rho^2}{[\xi^2(\mathbf{k}) + \rho^2]^{3/2}} \tanh \frac{\sqrt{\xi^2(\mathbf{k}) + \rho^2}}{2T} - \frac{\xi^2(\mathbf{k})}{2T[\xi^2(\mathbf{k}) + \rho^2]} \frac{1}{\cosh^2 \frac{\sqrt{\xi^2(\mathbf{k}) + \rho^2}}{2T}}, \end{aligned} \quad (\text{A.11})$$

$$\begin{aligned} T \sum_{n=-\infty}^{\infty} \text{Tr}[\mathcal{G}(i\omega_n, \mathbf{k}) \hat{I} \mathcal{G}(i\omega_n, \mathbf{k}) \hat{I}] &= 2T \sum_{n=-\infty}^{\infty} \frac{\xi^2(\mathbf{k}) + \rho^2 - \omega_n^2}{[\omega_n^2 + \xi^2(\mathbf{k}) + \rho^2]^2} \\ &= -\frac{1}{2T} \frac{1}{\cosh^2 \frac{\sqrt{\xi^2(\mathbf{k}) + \rho^2}}{2T}}, \end{aligned} \quad (\text{A.12})$$

where the Green function  $\mathcal{G}(i\omega_n, \mathbf{k})$  is given by (3.4). Both formulas can easily be calculated using Eq. (A.7) and its derivative with respect to  $c$ .

## REFERENCES

- \* E-mail: [vgusynin@bitp.kiev.ua](mailto:vgusynin@bitp.kiev.ua)
- † E-mail: [vlloktev@bitp.kiev.ua](mailto:vlloktev@bitp.kiev.ua)
- ‡ On leave from Bogolyubov Institute for Theoretical Physics, National Academy of Sciences of Ukraine, 252143 Kiev, Ukraine
- [1] V. M. Loktev, Fiz. Nizk. Temp. **22**, 3 (1996) [Low Temp. Phys. **22**, 1 (1996)].
- [2] M. Randeria, Varena Lectures, 1997, Preprint cond-mat/9710223.
- [3] Y. J. Uemura, Preprint cond-mat/9706151, to be published in Physica C.
- [4] M. Randeria, in *Bose Einstein Condensation*, A. Griffin, D. W. Snoke, and S. Stringari (eds.), Cambridge U. P., New York (1995) p. 355.
- [5] R. Haussmann, Phys. Rev. B **49**, 12975 (1994).
- [6] E. V. Gorbar, V. M. Loktev, and S. G. Sharapov, Physica C **257**, 355 (1996).
- [7] E. V. Gorbar, V. P. Gusynin, and V. M. Loktev, Fiz. Nizk. Temp. **19**, 1171 (1993) [Low Temp. Phys. **19**, 832 (1993)]; Superconductivity: Physics, Chemistry, Technology **6**, 375 (1993); Preprint ITP-92-54E, Kiev, 1992.
- [8] N. D. Mermin, H. Wagner, Phys. Rev. Lett. **17**, 1113 (1966);  
P. C. Hohenberg, Phys. Rev. **158**, 383 (1967);  
S. Coleman, Comm. Math. Phys. **31**, 259 (1973).
- [9] S. Schmitt-Rink, C. M. Varma, and A. E. Ruckenstein, Phys. Rev. Lett. **63**, 445 (1989).
- [10] J. Serene, Phys. Rev. B **40**, 10873 (1989).
- [11] A. Tokumitsu, K. Miyake, and K. Yamada, Phys. Rev. B **47**, 11988 (1993).
- [12] P. Nozières and S. Schmitt-Rink, J. Low. Temp. Phys. **59**, 195 (1985).
- [13] S. V. Traven, Phys. Rev. Lett. **73**, 3451 (1994).
- [14] R. MacKenzie, P. K. Panigrahi, and S. Sakhi, Int. J. Mod. Phys. A **9**, 3603 (1994);  
Phys. Rev. B **48**, 3892 (1993).
- [15] M. Drechsler and W. Zwerger, Ann. Phys. (Germany) **1**, 15 (1992).
- [16] S. Stintzing and W. Zwerger, Phys. Rev. B **56**, 9004 (1997).
- [17] V. M. Loktev and Yu. G. Pogorelov, Physica C **272**, 151 (1996).
- [18] D. Pines, J. of Physics **20**, 535 (1996).
- [19] H. Ding, T. Yokoya, I. C. Campuzano et al., Nature **382**, 51 (1996).
- [20] V. P. Gusynin, V. M. Loktev, and S. G. Sharapov, JETP Lett. **65**, 182 (1997);  
Fiz. Nizk. Temp. **23** 1247 (1997) [Low Temp. Phys. **23**, 936 (1997)].
- [21] H. Kleinert, Fortschritte Physik **26**, 565 (1978).
- [22] E. Witten, Nucl. Phys. B **145**, 110 (1978).
- [23] I. J. R. Aitchison, P. Ao, D. J. Thouless, and X.-M. Zhu, Phys. Rev. B **51**, 6531 (1995).
- [24] M. Capezzali, D. Ariosa, and H. Beck, Physica B **230-232**, 962 (1997).
- [25] Yu. A. Izyumov and Yu. N. Skryabin, *Statistical Mechanics of Magnetically Ordered Systems*, [in Russian], Nauka, Moscow (1987), Ch. 15.
- [26] P. Minnhagen, Rev. Mod. Phys. **59**, 1001 (1987).
- [27] V. Emery and S. A. Kivelson, Nature **374**, 434 (1995); Phys. Rev. Lett. **74**, 3253 (1995);  
Preprint cond-mat/9710059.
- [28] S. Doniach and M. Inui, Phys. Rev. B **41**, 6668 (1990).
- [29] A. M. J. Schakel, Mod. Phys. Lett. B **4**, 927 (1990).
- [30] O. Tchernyshyov, Phys. Rev. B **56**, 3372 (1997).
- [31] B. Janko, J. Mali, and K. Levin, Phys. Rev. B **56**, 11407 (1997).

- [32] J. R. Engelbrecht, A. Nazarenko, M. Randeria, and E. Dagotto, Preprint cond-mat/9705166.
- [33] K. Miyake, Progr. Theor. Phys. **69**, 1794 (1983).
- [34] H. Yamamoto and I. Ichinose, Nucl. Phys. **B370**, 695 (1992).
- [35] V. M. Loktev and S. G. Sharapov, Fiz. Nizk. Temp. **23**, 180 (1997) [Low Temp. Phys. **23**, 132 (1997)].
- [36] M. Casas, J. M. Getino, M. de Llano et al., Phys. Rev. B **50**, 15945 (1994).
- [37] D. van der Marel, Physica C **165**, 35 (1990).
- [38] A. V. Dotsenko and O. P. Sushkov, Preprint cond-mat/9601031.
- [39] T. P. Devereaux, Phys. Rev. Lett. **74**, 4313 (1995).
- [40] C. Kendziora et al., Phys. Rev. Lett. **77**, 727 (1996).
- [41] R. Micnas and T. Kostyrko, in *Proceedings of 1st Polish-US Conference*, Wroclaw, Poland, 11–15 September, 1995.
- [42] I. A. Kvasnikov, *Thermodynamic and Statistical Physics* [in Russian], Moscow University Press, Moscow (1991).
- [43] J. J. Deisz, D. W. Hess, and J. W. Serene, Preprint cond-mat/9706012.
- [44] A. A. Abrikosov, L. P. Gorkov, and I. E. Dzyaloshinski, *Methods of Quantum Field Theory in Statistical Physics*, Dover, New York, (1975).

## FIGURE CAPTION

FIG. 1.

$T_{\text{BKT}}$  and  $T_\rho$  versus the noninteracting fermion density. Dots represent the function  $\rho(\epsilon_F)$  at  $T = T_{\text{BKT}}$ . The regions of normal phase (NP), pseudogap phase (PP), and BKT phase are indicated.

FIG. 2.

$\mu(T)$  for various values of  $\epsilon_F/|\epsilon_b|$ : 1) 0.05; 2) 0.2; 3) 0.45; 4) 0.6; 5) 1; 6) 2; 7) 5. (For  $\mu > 0$  and  $\mu < 0$  the chemical potential was scaled to  $\epsilon_F$  and  $|\epsilon_b|$ , respectively.) The thick lines delimit regions of BKT, pseudogap (PP), and normal (NP) phases.

FIG. 3.

$2\Delta/T_{\text{BKT}}$  and  $2\Delta/T_\rho$  versus the non-interacting fermion density.

FIG. 4.

Phase diagram of the 2D metal at low concentrations. The dotted line corresponds to  $\mu = 0$ , and the temperature  $T_P$  separates abnormal normal phase (ANP) from normal phase. The critical temperature  $T_{\text{BKT}}$  is not shown.

FIG. 5.

$\chi(T)$  for various values of  $\epsilon_F/|\epsilon_b|$ : 1) 0.6; 2) 1; 3) 5; 4) 10; 5) 30.

# FIGURES

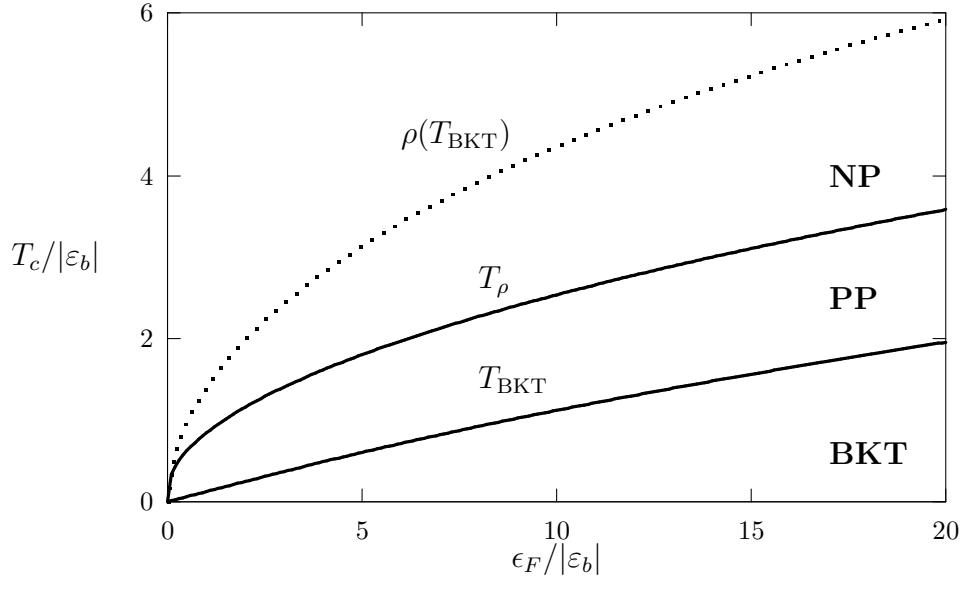


FIG. 1.

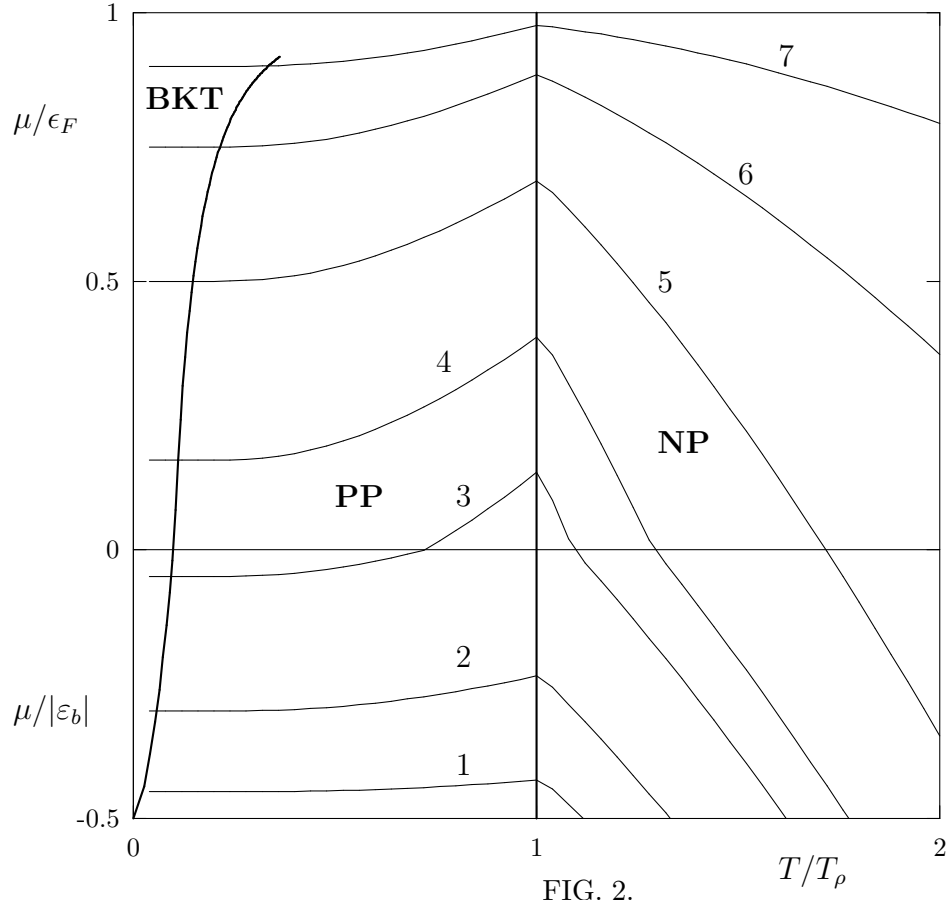


FIG. 2.

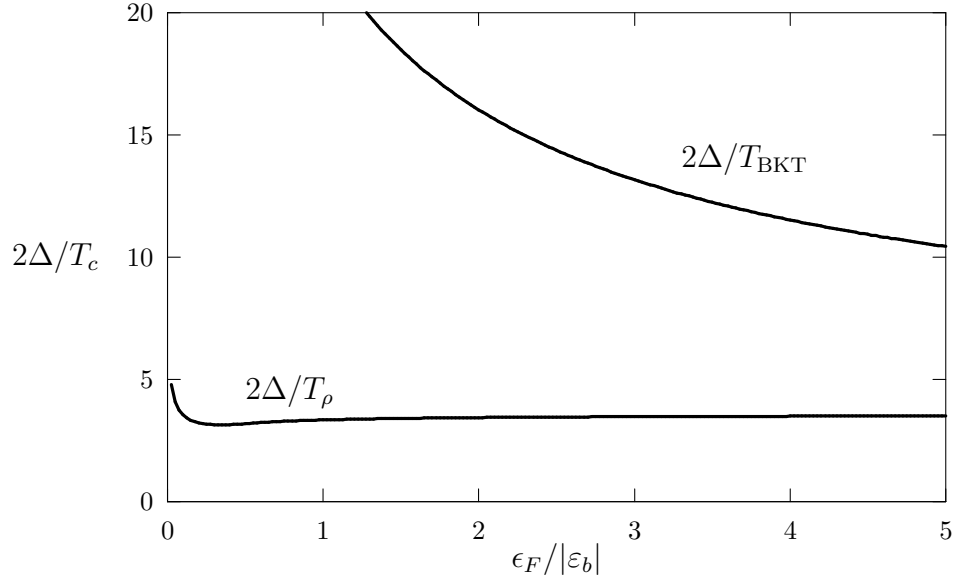


FIG. 3.



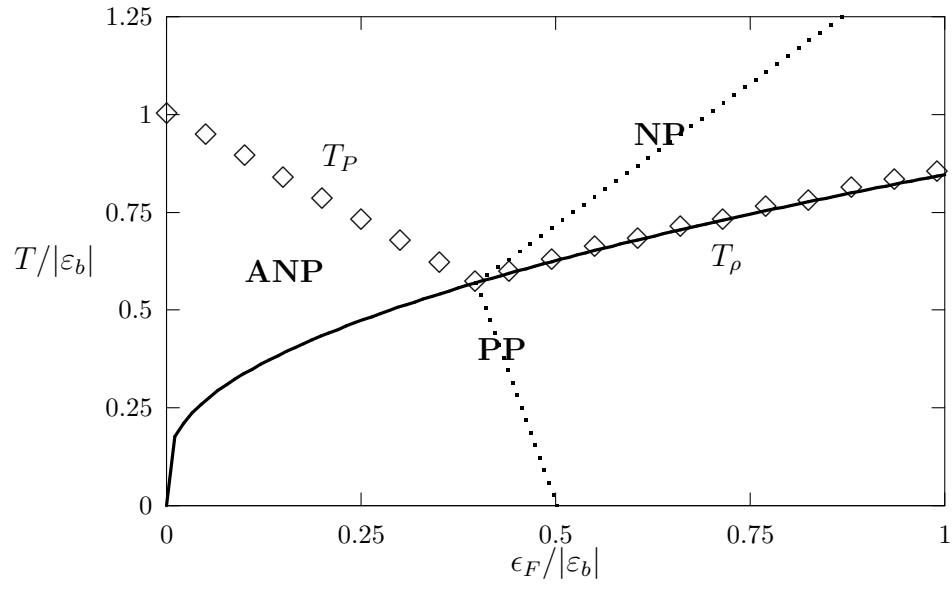


FIG. 4.

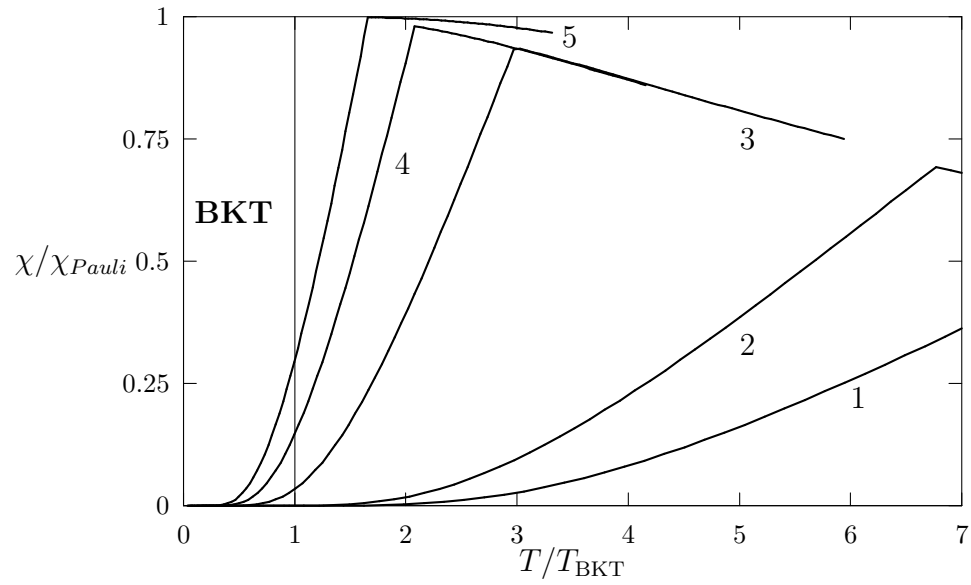


FIG. 5.